

THE EFFECT OF INCORPORATION OF DIFFERENT CARBON NANOTUBES ON THE PROPERTIES OF POLYPYRROLE NANOCOMPOSITE – MOLECULAR MODELING AND EXPERIMENTAL INVESTIGATIONS

L. PILAN^a, M. RAICOPOL^a, E. VASILE^b, M. IONITA^{a*}

^a*University Politehnica of Bucharest, Bucharest, 060042, Romania*

^b*Metav-CD, Bucharest, 020011, Romania*

A computational routine, based on atomistic- and meso-scale simulations, and experiments were combined to assess the compatibility of polypyrrole (PPY) with single walled carbon nanotubes (SWCNTs), SWCNTs functionalized with carboxylic acid (COOH) or m-polyaminobenzene sulfonic acid (PABS) groups. Moreover the effect of different types of carbon nanotubes incorporation on the morphology and electrochemical response of PPY-SWCNTs-PABS and PPY-SWCNTs-COOH composites was investigated. Computational and experimental results clearly confirmed that SWCNTs-PABS are properly dispersed and have beneficial effect on PPY electroactivity and conductive properties. SWCNTs-COOH and SWCNTs were found to be difficult to incorporate within PPY matrix and exert just a marginal effect on the PPY properties.

(Received July 27, 2012; Accepted August 29, 2012)

Keywords: Molecular modelling, Polypyrrole, Single walled carbon nanotubes

1. Introduction

Conductive polymers have been an area of enormous interest over the past 30 years since the first discovery of conducting polyacetylene by Shirakawa et al. [1]. Extensive research on several conjugated polymers including poly(*p*-phenylene), polyaniline, polypyrrole (PPY), polythiophene, poly(*p*-phenylenevinylene) have led to their applications in rechargeable batteries, microelectronics, corrosion protecting, sensors or electrochromic displays [2-4]. Among the various conjugated polymers, PPY is one of the most promising, distinguished by outstanding conducting properties, chemical durability, and a relatively easy production process [3]. However, PPY presents wick mechanical properties which limit its applications [3]. The fascinating structural, mechanical and electronic properties of carbon nanotubes (CNTs) [5] have led to an explosion of research in nanoscience and nanotechnology [6]. Combining CNTs with conducting polymers is offering an attractive route to reinforce and introduce electronic properties based on morphological modification or electronic interaction between the two components [2-6]. The development of superior nanostructured composites depends on several factors including uniformity of dispersion, degree of alignment and the strength of polymer-carbon nanotubes interfacial bonding [2, 3, 7]. In the case of single walled carbon nanotubes (SWCNTs) their insolubility and poor compatibility with the polymers make the uniform dispersion within the polymer matrix very difficult, and the resulting inhomogeneous nanocomposites often have unsatisfying properties [8-9]. Their chemical modification can pave the way toward the synthesis of homogeneous polymer-CNTs composites [9-10]. In recent studies, we demonstrated that by combing polyaniline or epoxy resin with the suitable carbon nanotubes and by choosing the relative weight ratio carbon nanotubes/polymer the features of the resulting material can be finely

*Corresponding author: mariana.ionita@polimi.it

tuned [2-3, 11]. Conversely, we have shown that predictive modeling provides the opportunity to mutually understand better how composites behave in different conditions, to develop materials with enhanced performance for particular industrial applications and to limit the efforts of synthetic chemists in following the inefficient Edisonian prescription of creating all possible mixtures in order to isolate the desired materials. [2-3, 11-12]. Mesoscale simulations, particularly dissipative particle dynamic (DPD) has been demonstrated to accurately reproduce material morphology [13-14]. Although there are very few works reporting the computational characterisation of polymer/CNTs composites since performing these simulations is not a trivial task because of the significant number of beads involved, large equilibration times and the very complex chemical network structure [11-15].

In this work PPY-SWCNTs, PPY-SWCNTs functionalized with *m*-polyaminobenzene sulfonic acid (PABS) groups and PPY-SWCNTs functionalized with carboxylic acid (COOH) groups composite materials with different compositions were studied by atomistic- and meso-scale molecular modeling, physical-chemical and electrochemical techniques in order to assess composites morphology and electroactivity.

Our modeling routine is based on atomistic simulation to derive interaction energy values among all system components (PPY, SWCNTs, SWCNTs-COOH and SWCNTs-PABS); mapping of these values onto mesoscale simulation parameters; Flory-Huggins theory and mesoscopic simulations to determine system morphologies. Further experimental techniques were used for synthesis and characterization of the nanocomposite materials indicated to be the most promising by molecular modeling investigations.

2. Materials and method

2.1 Realisation of mesoscale bulk models

The molecular models construction and subsequent simulations were conducted using the Materials Studio 5.0 molecular modeling package of Accelrys [16]. In our DPD simulations a PPY monomer (pyrrol), a PABS monomer (*m*-aminobenzene sulfonic acid) and carboxylic group are represented with a single bead, each part separated by dashed circles (Fig. 1) is represented with a single bead. The considered PPY and PABS chains consisted of 50 and 10 beads, respectively. For SWCNTs mesoscale models six aromatic rings (Fig. 1d) were represented with a bead and each SWCNTs consisted of 16 beads. The beads of the same molecule are connected by harmonic spring having the spring constant $c = 4$.

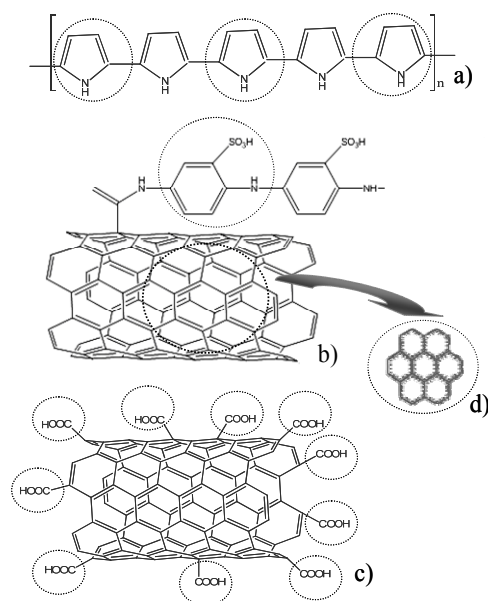


Fig. 1. DPD beads representation of PPY a), PABS b), COOH c) and SWCNTs d)

The nonbonded interactions acting between pairs of beads were determined employing atomistic simulations. Atomistic models of PPY, SWCNTs, SWCNTs-PABS, SWCNTs-COOH consisting of about 5000 atoms, within a periodic boundary condition box with lateral dimension of about 40 Å, were implemented and were subject of an intensive equilibration procedure. The molecular models construction and subsequent simulations were performed using COMPASS forcefield [17]. The methods used for models construction and equilibration is described in more detail elsewhere [2-3, 19]. Fig. 2 is a snapshot of the PPY atomistic bulk model during the last step of equilibration procedure. Afterwards the solubility parameters (δ) of composite system components were calculated employing Amorphous Cell Analysis modulus of the software using the Scatchard and Hildebrand theoretical treatments of mixing [19-20] and the values are listed in the Tab. 1.

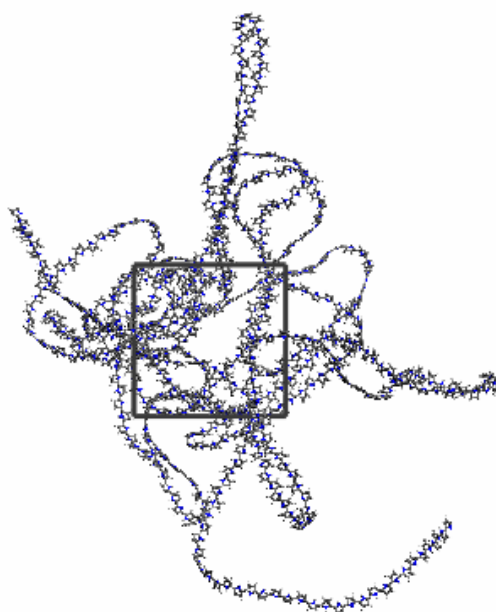


Fig. 2. PPY atomistic bulk model after refinement stage

Table 5. Solubility parameters and molar volume of composite systems components.

System component	Solubility parameter (δ) ((J/cm ³) ^{-0.5})	Molar Volume (cm ³ /mol)
PPY	16.04	75.53
SWCNT	13.15	110
COOH	20.08	89.44
PABS	18.08	43.02

Mesoscale, cubic models of PPY-SWCNTs, PPY-SWCNTs-COOH and PPY-SWCNTs-PABS were constructed with different compositions 98:2 and 95:5 (w/w) within a simulations box of 10×10×10 consisting of 3000 beads. In order to assess composite system morphology DPD calculations were run over 2×10⁵ steps with a time step of 0.05 reduced units (r.u.). As Groot and Warren suggested, density of the system was set to $\rho=3$ [21].

2.2 Experimental realisation of composite materials

The composite materials indicated to be the most promising by mesoscale simulations, *i.e.* PPY-SWCNTs-PABS and PPY-SWCNTs-COOH, were obtained as films and submitted for experimental characterisation. Pyrrole (Merck) was distilled and stored in the dark prior to use.

Other chemicals employed in this study were of reagent grade and were used without further purification. Aqueous solutions were prepared using distilled deionized water. The electrodeposition of nanocomposite films of PPY-SWCNTs-PABS and PPY-SWCNTs-COOH was done using galvanostatic method via co-deposition from a solution containing both the functionalized SWCNTs and the corresponding monomer (0.5M PPY). In a first step, the functionalized SWCNTs aqueous suspension (0.5 mg/mL) was prepared via sonication (1 hour) and then the pyrrole solution was prepared straightaway by dissolving the monomer in the nanotubes suspension. The PPY/Cl pure polymeric films were obtained from solutions of pyrrole of the same concentration containing 0.1M NaCl.

2.3 Experimental characterization of composite materials

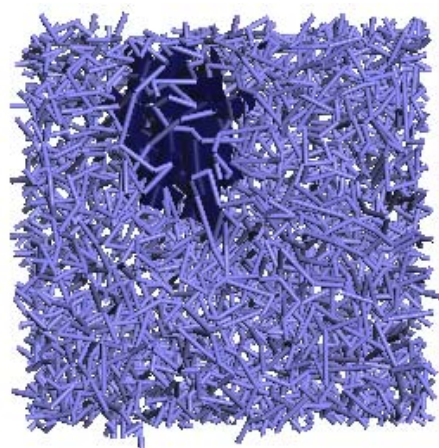
All electrochemical measurements were performed with a 128N Autolab potentiostat. A three-electrode configuration consisting of platinum (Pt, Metrohm, disks, diameter 2 mm) as working electrode, Hg/Hg₂Cl₂ (3M KCl) as reference electrode and a Pt wire as counter electrode was used. Cyclic voltammetry (CV) studies of the modified electrodes were performed in 0.1M NaCl solutions in the potential range -0.7 - 0.7 V at a scan rate of 0.1 Vs⁻¹. The morphology of the surface was assessed through scanning electron microscopy (SEM). The study was performed using a QUANTA INSPECT F SEM device equipped with a field emission gun (FEG) with 1.2 nm resolution and with an X-ray energy dispersive spectrometer (EDXT). To investigate the films by transmission electron microscopy (TEM), small pieces of film were taken from the surface of the substrate (Pt electrode) by scratching and deposited on a TEM copper grid covered with a thin amorphous carbon film with holes. High resolution transmission electron microscopy (HRTEM) investigations of the films structure were performed by using a TECNAI F30 G2 S-TWIN microscope operated at 300 kV with EDX and EELS facilities.

3. Results and discussion

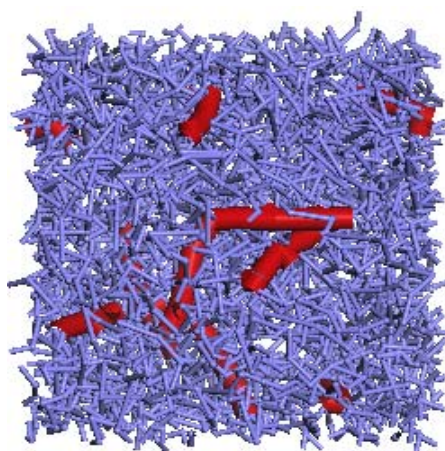
The present mesoscale simulation routine was focused to generate and characterize computational systems with large SWCNTs, SWCNT-PABS or SWCNTs-COOH weight fraction (2% and 5%). Although experimental systems typically contain much lower CNTs weight fraction, our simulation results can help to make useful prediction for lower CNTs weight fraction by extrapolation.

3.1 Prediction of models morphology

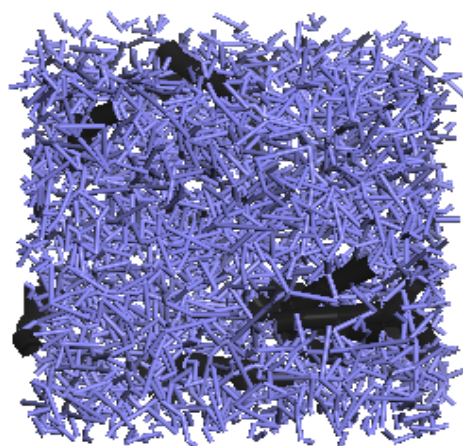
In order to analyze the SWCNTs, SWCNTs-COOH and SWCNTs-PABS dispersion within PPY matrix Flory-Huggins theory and DPD mesoscale technique were employed. A first morphology evaluation was performed assuming Flory-Huggins theory [22], which predicts that components with similar δ values lead to small repulsions and should mix, PPY ($\delta=16.04$ (J/cm³)^{0.5}) should mix well with SWCNTs-PABS ($\delta=18.08$ (J/cm³)^{0.5}) and reasonable with SWCNTs-COOH ($\delta=20.08$ (J/cm³)^{0.5}). In contrast, SWCNTs ($\delta=13.15$ (J/cm³)^{0.5}), which has a significantly different δ value, is expected not to form uniform composite with PPY. Fig. 3 illustrates the morphology of the three composite systems after $2 \cdot 10^5$ DPD calculation steps.



a)



b)



c)

Fig. 3. Equilibrium morphology of PPY-SWCNTs (95/5 w/w) a), PPY-SWCNTs-PABS (95/5 w/w) b) and PPY-SWCNTs-COOH (95/5 w/w) systems as modelled by DPD. SWCNTs are shown in dark blue, SWCNT-COOH are shown in black, SWCNTs-PABS are shown in red and PPY chains are shown in light blue.

At the beginning of the simulations, all the components were mixed together; after 5000 steps SWCNTs and PPY congregate, as expected according to Flory-Huggins theory. As the simulation time increases, formation of SWCNTs domains (Fig. 3a) was observed for both PPY-SWCNTs system compositions 98:2 and 95:5 (w/w). Fig. 3b illustrates the morphology of PPY-SWCNTs-PABS composite system. SWCNTs-PABS mix well with PPY polymeric chains, are

well embedded and singularly dispersed regardless of their concentration. SWCNTs-COOH are semidispersed within PPY matrix; some isolated nanotubes were blended with the matrix and wrapped by a thin layer of PPY, some other nanotubes form aggregates (Fig. 3c). The presence of aggregates of SWCNTs-COOH and SWCNTs is in line with Flory-Huggins theory which suggests a weak affinity with PPY, particularly between SWCNTs and PPY.

This observation was supported by SEM and TEM investigations which revealed for the PPY-SWCNTs-PABS composites a homogeneous structure with singularly dispersed and well embedded CNTs within the polypyrrole matrix (Fig. 4a). A good agreement between predicted material morphology and experimental data was found also for the material PPY-SWCNTs which presented aggregates of pristine SWCNTs in the composites (Fig. 4b). In what concerns PPY-SWCNTs-COOH nanocomposites was found that just short SWCNTs-COOH are incorporated and uniformly dispersed within PPY matrix (Fig. 4c). Uniform dispersion of carbon nanotubes in the PPY is a fundamental challenge. The effective utilization of SWCNTs in composite applications strongly depends on the ability to homogeneously disperse them throughout the PPY matrix. Given the molecular modeling indication further experimental investigation concerned just materials which presented an uniform distribution of carbon nanotubes *i.e.* PPY-SWCNTs-PABS and PPY-SWCNTs-COOH.

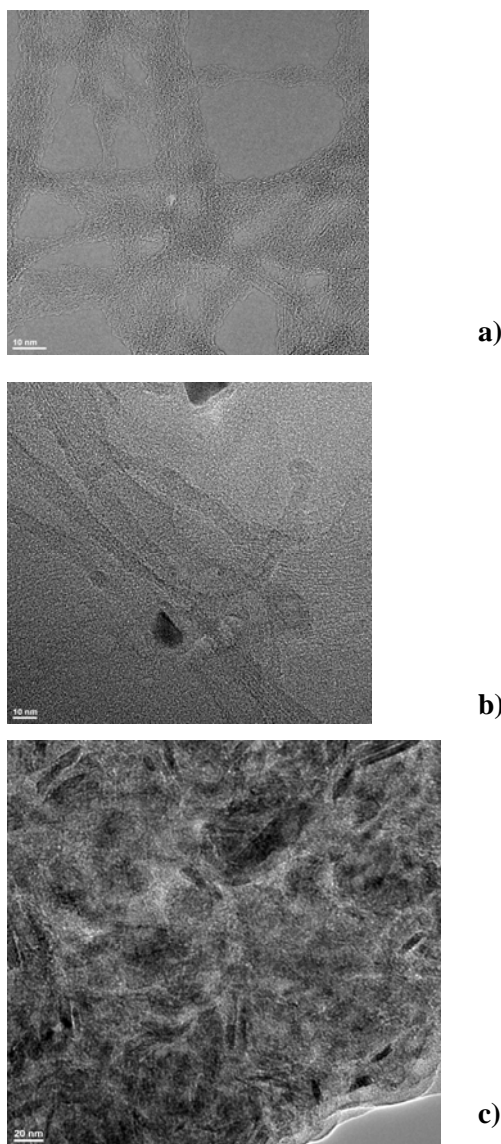


Fig. 4. TEM image of PPY-SWCNTs-PABS a), PPY-SWCNTs b) and PPY-SWCNTs-COOH c) nanocomposite.

3.2 Experimental characterisation of composite materials

The electroactivity of the pure PPY (Fig. 5 a) and the composite PPY films (PPY-SWCNTs-COOH (Fig. 5 b); PPY-SWCNTs-PABS Fig. 5 c) deposited for 900 mCcm^{-2} were studied in a monomer-free 0.1 M aqueous solution of NaCl. As can be seen from Fig. 5, each of the CVs shows a couple of broad cathodic and anodic peaks. The cathodic peak was found at about -0.2 to 0.4 V and the anodic peak was at about 0.1 to 0.3 V, indicating the insertion and expulsion of small cation ions of Na^+ . The difference between the CVs of pure PPY and PPY-SWCNTs-COOH is not significant, indicating that the electrochemical activity of these films results from its PPY component. The composite exhibit slightly higher currents than the pure polymeric ones, which can be translated into a larger capacitance of the former.

However, there are fundamental differences in the CVs characteristic for the PPY-SWCNTs-COOH and PPY-SWCNTs-PABS composite films. The first difference is that the PPY-SWCNT-PABS film is electrochemically active in a much wider potential window than PPY-SWCNTs-COOH film. The window in which PPY-SWCNTs-PABS is active ranges from -0.4 V, compared to -0.2 V for PPY-SWCNTs-COOH indicating that the presence of SWCNTs-PABS in PPY promotes the electron transfer of the redox processes. Secondly, the PPY-SWCNTs-PABS films exhibit higher currents than the other mentioned system, which can be translated into larger capacitance. The above observations indicate that the quantity of the functionalized SWCNTs entrapped in the PPY-SWCNTs-PABS is obviously higher than for PPY-SWCNTs-COOH film. This agrees very well with the TEM results which indicate numerous embedded SWCNTs-PABS within PPY matrix (Fig. 4a). Also, the voltammetric behaviour of the PPY/SWCNTs-PABS composite agrees very well with the SEM observations of the porous microstructures formed by the network of interconnected nano-fibrils. The capacitance of PPY-SWCNTs-PABS is larger than that of the pure polymeric PPY films because the mesoporous structure of SWCNTs-PABS makes the doping ions enter into/eject from PPY-SWCNTs-PABS composite films more easily.

The comparative stability upon cycling of the modified electrodes with approximately the same thickness can be also discussed. In contrast with the electrochemical response of the PPY/Cl film, the composite ones show less electroactivity loss.

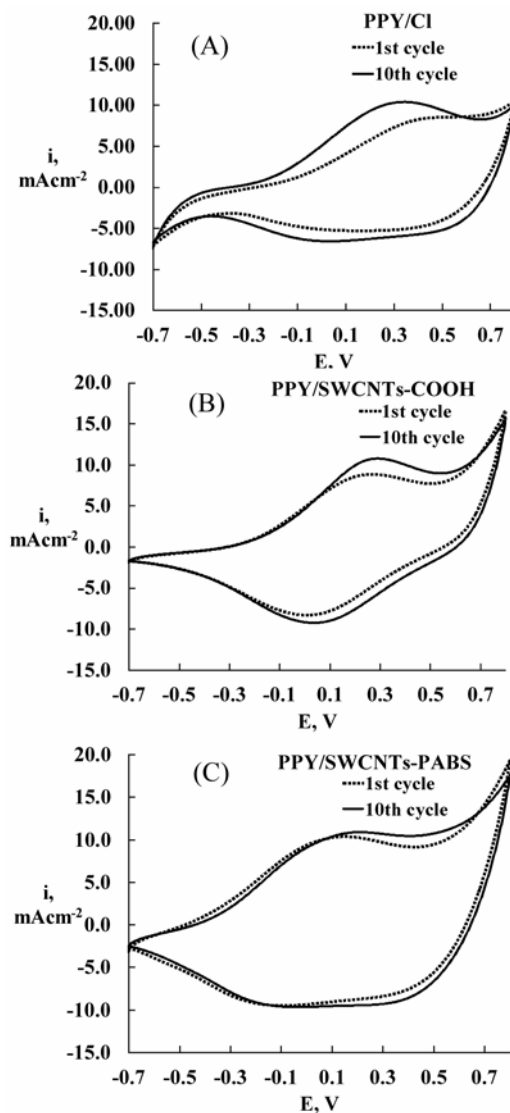


Fig. 5. Cyclic voltammograms at a scan rate of 0.1 V s^{-1} for PPY (A), PPY-SWCNTs-COOH (B), PPY-SWCNTs-PABS (C) (deposited for 900 mCcm^{-2}) in 0.1 M aqueous solution of NaCl

The current intensity remains almost unchanged after 10 cycles for the PPY-SWCNTs-PABS composite films, in contrast with the gradual decrease observed for the pure polymeric one.

In Fig. 6 the SEM images for PPY pure polymeric film and PPY-SWCNTs-PABS composite film are comparatively presented. The morphology of the PPY-SWCNTs-PABS composites consists in a three-dimensional network composed of interconnected fibrils with diameters in the range of 50–300 nm. The diameter of the PPY-SWCNTs-PABS fibrils is significantly larger than that of the functionalized SWCNTs and this indicates a good interaction between the SWCNTs-PABS dopant and pyrrole monomer. The functionalized SWCNTs acted both as a dopant and also provided a large surface area for the polymerization process to take place. We can say that the three-dimensional network was formed with the functionalized SWCNTs serving as the backbone, thus greatly electroactive properties of the composite film. The improved electrochemical properties for the PPY-SWCNTs-PABS film can be also explained by this porous morphology of the composite film that provides enough pathways for the movement of ions and solvent molecules within the film. The current intensity remains almost unchanged after 10 cycles for the PPY-SWCNTs-PABS composite films, in contrast with the gradual decrease observed for the pure polymeric one.

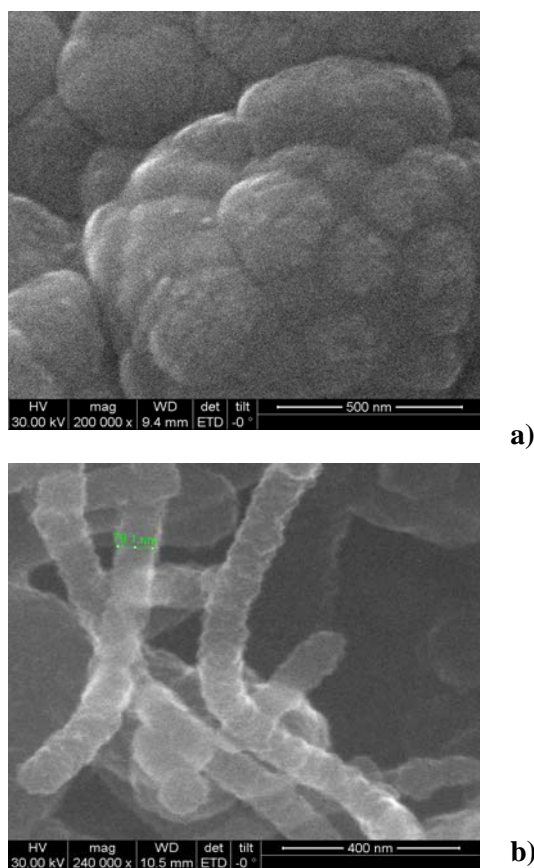


Fig. 6. SEM images of the film surface for a) PPY/Cl and b) PPY-SWCNTs-PABS (film-formation charge 900 mC/cm^2).

4. Conclusion

It was shown that DPD simulations combined with experimental tests are an effective methodology, providing information on phenomena that take place at mesoscale level, determining the macroscale properties of a given material. Therefore, joining molecular modeling to the experimental work would help to conduct more focused and model-oriented tests, avoiding the time-consuming trial-and-error procedure.

The computational routine based on atomistic- and meso-scale simulations allows to achieve well equilibrated bulk models and to predict PPY-SWCNTs, PPY-SWCNTs-PABS and PPY-SWCNTs-COOH composite systems morphology accurately.

The simulation results suggested the possibility to uniform and singularly disperse SWCNTs-PABS within PPY. Among the studied composite systems PPY-SWCNTs-PABS exhibited the highest capacitance, electrochemical activity and stability.

Instead incorporation of SWCNTs or SWCNTs-COOH generates just a marginal effect on composite properties due to weak interfacial adhesion with PPY chains, low incorporation level and their tendency to agglomerate.

Acknowledgements

This research has been supported by the National Research Grant PN-II-RU-TE-_153, CNCS-UEFISCDI.

References

- [1] H. Shirakawa, E. J. Louis, A. G. MacDiarmid, C. K. Chiang, A. J. Heeger. *J. Chem. Soc., Chem. Commun.* 578 (1977).
- [2] M. Ionita, V. Ciupina, E. Vasile, *J. Optoelectron. Adv. M.* **13**, (2011).
- [3] M. Ionita, A. Pruna, *Prog. Org. Coat.* **72**, (2011).
- [4] A. Pud, N. Ogurtsov, A. Korzhenko, G. Shapoval. *Prog. Polym. Sci.* **28**, (2003).
- [5] S. Ijima. *Nature* **354**, 56 (1991).
- [6] J. Anand, S. Palaniappan, D. N. Sathyanarayana. *Prog. Polym. Sci.* **23**, 993 (1998).
- [7] J. Gou, B. Minaie, B. Wang, Z. Liang, C. Zhang, *Comp. Mater. Sci.* **31**, (2004).
- [8] A. Peigney, E. Flahaut, C. Laurent, F. Chastel, A. Rousset. *Chem. Phys. Lett.* **352**, (2002).
- [9] A.B. Dalton, C. Stephan, J.N. Coleman, *J. Phys. Chem. B.* **10**, (1998).
- [10] J.L. Bahr, J. Yang, D.V. Kosynkin, *J. Am. Chem. Soc.* **123**, (2001).
- [11] M. Ionita, *Compos. Part B Eng.* (2012), doi.org/10.1016/j.compositesb.2011.12.008
- [12] M. Ionita, H. Iovu, *Compos. Part B Eng.* **43**, (2012),
- [13] A. Maiti, J. Wescott, P. Kung, G. Goldbeck, *Int. J. Nanotech.* **2**, (2005).
- [14] A. Maiti, J. Wescott, P. Kung, *Mol. Sim.* **31**, (2005).
- [15] A. Gautieri, M. Ionita, D. Silvestri, E. Votta, S. Vesentini, G.B. Fiore, N. Barbani, G. Ciardelli, A. Redaelli, *J. Comput. Theor. Nanosci.* **7**, (2010).
- [16] Materials Studio 5.0 software (Accelrys, Inc. UK) tutorial.
- [17] H. Sun H. J. *Phys. Chem. B.* **102**, (1998).
- [18] D. Hofmann, L. Fritz, C. Ulbrich, C. Schepeers, M. Bohning, *Macromol. Theory Simul.* **9**, (2000).
- [19] S.G. Scatchard, *Chem. Rev.* **8**, (1931).
- [20] J.H. Hildebrand, *J. Am. Chem. Soc.* **38**, (1916).
- [21] R.D. Groot, P.B. Warren, *J. Chem. Phys.* **107**, (1997).
- [22] P.E. Rouse, *J. Chem. Phys.* **21**, (1953).